

Preparation of Polymer Inclusion Membranes (PIMs) with Ionic Liquid and its Application in Dye Adsorption Process Supported by Statistical Analysis

D. Shanthana Lakshmi^{1,3,*}, Sergio Santoro¹, Elisa Avruscio², Antonio Tagarelli² and Alberto Figoli^{1,*}

¹Institute on Membrane Technology, ITM-CNR, via P. Bucci, cubo 17/C, 87030 Rende (CS), Italy

²Chemistry and Chemical Technologies Department, University of Calabria, 12c, 87030 Rende (CS), Italy

³Reverse Osmosis Division CSIR-Central Salt and Marine Chemicals Research Institute (CSIR-CSMCRI), G. B. Marg, Bhavnagar- 364002, (Gujarat), India

Abstract: Polymer inclusion membranes (PIMs) were prepared via Non-Solvent Induced Phase Separation (NIPS) using polyethersulfone (PES) loaded with a liquid ionic, 1-butyl-3-methylimidazolium hexafluorophosphate ([BMIM][PF6]). Hydrophilic porous PIMs with a controlled morphology were obtained and tested for the removal of reactive blue 19 (RB19) as a model anionic dye. The dye adsorption efficiency depends on several variables *i.e.* pH, contact time, initial dye concentration, amount and weight of adsorbent (PIMs). The optimal values of these parameters were calculated by the multivariate approach of "Experimental design" and, in particular, a central composite design (CCD). The optimal conditions obtained from the response surface data are: [BMIM][PF6] concentration 10.7wt%, pH 3.0, RB19 dye concentration 10.0 ppm and PIMs of weight 0.055 mg. The experimental adsorption percentage of RB19 value (69.2%) was in agreement to those predicted by the CCD model (71.7%).

Keywords: Ionic liquid, Polymer inclusion membranes (PIMs), Dye Adsorption, Central Composite Design (CCD).

1. INTRODUCTION

The treatment of wastewaters containing dye residue from several industries (*i.e.* textile, printing, and ink) is in an alarming stage because of its impact on the environmental pollution [1-3]. The effluent of these industries were discarded into rivers or lakes altering the natural equilibrium as a consequence of the toxicity of the dye and the reduction of the photosynthetic activity due to the colourization of the water [4-6]. Due to its resistance towards biological degradation, conventional biological treatment is not efficient to treat dye effluent. Several chemical-physical methods are developed for dye removal such as coagulation/flocculation, ozone treatment, chemical oxidation, adsorption, photocatalytic and membrane process [7]. Adsorption has been considered as an economical, simple and efficient technique to treat effluent [8-10]. The disadvantage of adsorption is the need to regenerate adsorbent and time required for adsorption process, which will increase the cost of the process. As reported in the literature, the performance of different adsorbents in dye removal are activated carbons, zeolites, activated clay, activated slag, chitosan beads, cellulosic resins, polymer resins, modified cross-linked starch, red mud, bottom ash and de-oiled soya [11-23].

Quite recently, ionic liquids (ILs) have been extensively investigated as promising chemical enable to replace solvent in different processes, such as water treatment or clean synthesis/extraction [24]. ILs are salts existing as liquid at room temperature mainly composed of organic cations (*i.g.* imidazolium, pyridinium, pyrrolidinium, ammonium or phosphonium) and either organic or inorganic anions (*i.g.* acetate, trifluoroacetate, tetrafluoroborate, hexafluorophosphate or bromide anions) [25]. ILs show exceptional properties such as negligible vapour pressure, thermal stability, miscibility with a wide range of organic solvents, good extractability for many different organic, inorganic and organometallic materials, tunable chemical structure and physical properties [26-29]. Several ILs were found to be perfect solvents for water-soluble dyes separation in aqueous phase, such as [BMIM][PF6], 1-hexyl-3-methylimidazolium hexafluorophosphate ([HMIM][PF6]), 1-hexyl-3-methylimidazolium tetrafluoroborate ([HMIM][BF4]) [30].

The disadvantage of these techniques is that the removal and recovery of ILs and additional treatments require cost in the process of wastewaters purification and develop burden on its commercial scale applications. For this reason, IL could be incorporated into a solid support that facilitate the handling of the adsorbent and its removal from wastewater. Supported

*Address correspondence to this author at the ITM-CNR, Rende Italy;
Tel: +39-098492027; Fax: +39-0984402103;
E-mail: slakshmi@csmcri.org; a.figoli@itm.cnr.it

liquid membranes (SLMs) consist of porous support impregnated with solvent/extractant, have been considered as a potential technique to remove contaminants from wastewater; such as: chemical precipitation, coagulation–flocculation, flotation, ion-exchange, electro-oxidation and adsorption [31-34].

The main drawback of SLMs is their poor stability limiting their employment in particular in large-scale applications [35]. For this reason, several works have been dedicated on the development of polymer inclusion membranes (PIMs), formed by casting a solution containing an extractant a base polymer. The basic principle is similar to SLMs, the role of the polymer is to entrap the active component of the membrane and minimize any loss of in the solution, but it is notorious that PIMs exhibit better mechanical properties and chemical resistance than traditional SLMs since in the former the carrier is immobilized onto a polymer matrix [36-40]. However, the included chemical might affect not solely the transport properties of the polymer, but also the morphology and the chemical-physical properties of the membrane.

PIMs loaded with conventional chemical complexing agents (D2EHPA, TOA) were explored for dye removal from aqueous streams. Adsorbents loaded liquid membranes (emulsion, supported, hollow fiber types) and molecular imprinted membranes were tested for dye removal process [41-42]. Removal of red acid dye performed with a PIM of cellulose triacetate (membrane matrix material) embedded with the carrier tricaprilmethylammonium chloride (Aliquat 336) and using 2-nitrophenyl octyl ether, as plasticizer [43-46]. Effect of aqueous phase pH, concentration of extractant (Aliquat336) in the membrane, initial dye concentration and stirring speed were the crucial factor in dye removal efficiency. Mansoureh Zarezadeh-Mehrizi group [47] reported N-methyl-N'-propyl trimethoxy silylimidazolium chloride functionalized into nanoporous silica for removal of anionic dye methyl orange. Azodyes were successfully extracted into an IL, N-butyl-N-methyl pyrrolidinium bis (trifluoromethanesulfonyl) amide ([P14][Tf2N]), with an efficiency of 98% [48]. Reactive dyes were removed from aqueous solution by the mechanism of ion-exchange due to the addition of dicyclohexyl-18-crown-6 coupled with ionic liquid [49]. Several ILs were found to be perfect solvents for water-soluble dyes separation in aqueous phase, such as [BMIM][PF6], 1-hexyl-3-methylimidazolium hexafluorophosphate ([HMIM][PF6]), 1-hexyl-3-methylimidazolium tetrafluoroborate ([HMIM][BF4]) [50-51].

The current investigation refers to the evaluation of the dye adsorptive performance of [BMIM][PF6] loaded polyethersulfone (PES) polymer inclusion membranes (PIMs). Membranes were prepared via Non-Solvent Induced Phase Separation (NIPS) using dimethylsulphoxide (DMSO), as non-toxic solvent [29], Poly-N-vinyl pyrrolidone (PVPK17) as pore former and varying the polymeric dope composition to prepare membrane suitable for dye removal application. PVPK17 enhances the liquid-liquid demixing rate during the precipitation of the polymer in water because of its high hydrophilicity [52]. PES is an inexpensive polymer generally used for the preparation of microfiltration (MF), ultrafiltration (UF) and gas separation membranes because of chemical and thermal properties (wide range of temperature and pH of workability, chemical resistance (aliphatic hydrocarbons, alcohols, chlorine and acids) useful in membrane preparation in different configurations with tailored pore sizes available for UF and MF applications ranging [53-54]. In this work, an anionic reactive blue 19 (RB19) dye was selected due to its toxicity and recalcitrant nature. The efficiency of the dye adsorption process is influenced by several parameters, such as dye, IL adsorbent concentration and aqueous phase pH. The multivariate approach of "experimental design" was used to identify the optimal conditions to maximize the performance of the process in term of dye removal.

2. MATERIALS AND METHODS

2.1. Material

Polyethersulfone (PES) from ICI Victrex used as a polymer to prepare membranes. Poly-N-vinylpyrrolidone (PVPK17) Luviskol® K-17 Pulver (Mw 7–11kDa) (BASF, Germany), Dimethylsulphoxide (DMSO EVOL, Arkema, France) and Isopropanol (IPA) (Carlo Erba Reagents, Sigma-Aldrich, Italy), 1-butyl-3-methylimidazolium hexafluorophosphate ([BMIM][PF6]) (Iolitec-Ionic Liquid Technologies, Germany) were purchased and used as received. Reactive Blue 19/ Remazol Brilliant Blue R (Colour Index Number: 61200, chemical formula: $C_{22}H_{16}N_2Na_2O_{11}S_3$, MW: 626.54 g mol⁻¹, λ_{max} : 598 nm) was purchased by Sigma-Aldrich and was used without purification. Double distilled water was used throughout.

2.2. Membrane Preparation

PES powder was dissolved in DMSO at different concentration (from 10wt% to 15wt%). The mixture was kept under magnetic stirring at 50°C for about 24 hours until the PES complete solubilisation. Subsequently,

PVPK17 was added to the polymeric solution (from 0wt% to 4wt%) followed by [BMIM][PF6] (from 0wt% to 25wt%). The dope was kept under magnetic stirring at 50°C until the mixture was homogeneous. In the case of a dope solution prepared with the higher concentration of 25wt% of IL, the viscosity of the mixture was too high that the increase of temperature from 50°C to 80°C was required. Afterward, the stirring was stopped, and the polymeric solution was kept at constant temperature (50°C) overnight to release the gas bubbles. The casting solution was cast onto a glass plate at 25°C using a hand casting knife with a gap of 450 µm and then immersed into a coagulation bath of 50wt%IPA-50wt% H₂O for 24 hr to promote the complete coagulation of the membrane. The membrane was removed from coagulation bath and washed and soaked in distilled water for 48 hr to remove the PVPK17 and solvent residues. Flat sheet PES PIMs were dried at 50°C in a vacuum oven for 24 hr. The several compositions of the dope solution, used to prepare the polymer inclusion membranes (PIMs) of PES, are displayed in Table 1.

2.3. Characterization

Membranes cast with PES/ [BMIM][PF6]/PVPK17 (PIM) and blank PES membranes were characterized by several conventional techniques.

a) *Thickness*: The thicknesses of produced PIMs membranes were evaluated by means of a digital micrometer with a precision of ±0.0001 mm (Carl Mahr D 7300, Esslingen AN, Gottingen, Germany). For each membrane, ten measurements were taken.

b) *SEM analysis*: The surface morphology of produced membranes was observed by scanning electron microscope (SEM; Steroscan 360, Cambridge Instruments, Cambridge, UK) at 20 kV and cross-section samples were freeze fractured in liquid nitrogen to produce a clean brittle fracture. Samples were sputter coated with gold for 180 s using a sputter current of 130 mA (Q150T ES Turbo-Pumped Sputter Coater/Carbon Coater, Quorum Technologies, Ltd, Laughton, UK).

c) *Bubble point and pore size*: Membrane bubble point and pore size were measured by using a PMI Capillary Flow porometer (Porous Materials Inc., USA) following the procedure described in literature [55]. Briefly, the membranes were immersed for 24 hours in Pore wick (16 dyne/cm). Samples were placed in the membrane cell of the porometer and tests were performed according to the wet-up/dry-up mode using the software Capwin, consisting in increasing the pressure in one of the compartment of the cell in order

Table 1: Polymer Dope Solution Composition used to Prepare PES- PIMs

Polymer Dope Solution	PES (wt%)	DMSO (wt%)	PVPK 17 (wt%)	[BMIM][PF ₆] (wt%)
1	10	90	0	0
2	10	88	2	0
3	10	83	2	5
4	10	73	2	15
5	10	63	2	25
6	10	86	4	0
7	10	81	4	5
8	10	71	4	15
9	10	61	4	25
10	15	85	0	0
11	15	83	2	0
12	15	78	2	5
13	15	68	2	15
14	15	58	2	25
15	15	81	4	0
16	15	76	4	5
17	15	66	4	15
18	15	56	4	25

to remove the liquid from the pores and in repeating the experiment with dried membranes. The measurement of bubble point, largest pore size and pore size distribution is based on the Laplace's equation:

$$d_p = \frac{4 \pi \cos \theta}{p} \quad (1)$$

where d_p is the pore diameter, τ is the surface tension of the liquid, θ is the contact angle of the liquid (assumed to be 0 in case of full wetting, which means $\cos \theta = 1$) and P is the external pressure. The results were processed using the software Caprep for further processing. For each sample, two measurements were taken; the average value and the corresponding standard deviation were, then, calculated.

e) *Porosity*: Membrane porosity was determined by the gravimetric method. Measurements were carried out by weighing the membrane in dry and wet condition (24 hr in kerosene). The overall porosity was calculated according to the following equation [56]:

$$\varepsilon = \left\{ \frac{(w_1 - w_2)/D_k}{(w_1 - w_2)/D_k + w_2/D_p} \right\} \quad (2)$$

where w_1 is the weight of the wet membrane; w_2 is the weight of the dry membrane; D_k is the kerosene density (0.82 g cm^{-3}) and D_p is the polymer density (1.45 g cm^{-3}). For each membrane, 3 measurements were performed; the average value and the corresponding standard deviation were, then, calculated.

f) *Contact angle*: The contact angles (CA) with distilled water on both the surfaces were measured by

the sessile drop method at ambient temperature using CAM 200 contact angle meter (KSV Instruments, Finland). The average value and the corresponding standard deviation were calculated after taken 10 measurements.

g) *Water permeability*: The schematic representation of the set-up used to carry out the measurement of water permeability is shown in Figure 1. It consists of an analytic balance (Europe 6000, Gibertini), peristaltic pump (ABB IP 20/UL Open Type), thermostatic bath (Thermo Electron; type 003-2859) and dead-end type membrane cell (Membrane area $0,044 \text{ m}^2$).

Water permeability (P_e) measurements were carried out by feeding distilled water into the system (temperature 25°C) at three different feed pressures (0.5, 1.0 and 1.5 bar). Thermocouples (accuracy: $\pm 0.1^\circ\text{C}$) were used to detect temperature variation in the feed and the amount of permeate was evaluated by mass difference. Three experiments were performed for each conditions and each membrane.

2.4. Reactive Blue19 Dye Adsorption Batch Tests

Experiments of RB19 dye adsorption in the batch were performed in the operative conditions suggested by experimental design (Taguchi method) and literature review. Stock solutions of Reactive Blue 19 were prepared in distilled water by adjusting the required pH (with 0.1M HCl or 0.1M NaOH). The stock solutions were prepared by changing the pH (from 3 to 10) and dye concentration (from 10 ppm to 30 ppm).

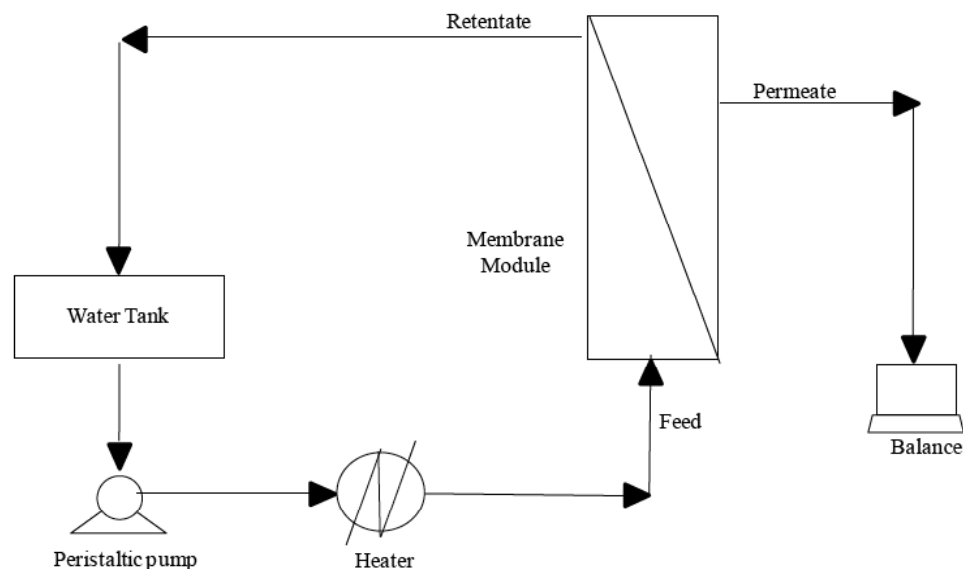


Figure 1: Scheme of the set-up used to measure water permeability.

Experiments were performed in 50 mL flask into which 40 ml dye aqueous solution and a known weight of PES membranes were added (from 0,02g to 0,06g). The samples were kept under stirring at 25°C. The concentration of the residual RB19 was analyzed by UV-vis spectrophotometer (UV-160A Shimadzu) at 598 nm corresponding to the maximum absorbance of the dye.

The percentage of RB19 removal (R) is related to the adsorption capacity of PIM and blank PES was calculated at various conditions by using the following equation:

$$R = \frac{(A_0 - A_t)}{A_0} \% \quad (2)$$

where, A_0 is initial absorbance of the batch and A_t is its concentration at time t. Experiments were repeated at least two times.

3. RESULTS AND DISCUSSION

3.1. Membrane Characterization Results

The membranes prepared with PES / PVPK17 / [BMIM][PF6] and blank PES (PES / PVPK17) were characterized by conventional analytical tools (SEM,

Thickness, Porosity, Contact angle, permeability, etc.) and summarized in Table 2.

3.1.1. Membrane morphology –SEM Analysis

The morphologies of the PES and PIM ([BMIM][PF6] loaded) membrane surface and cross section images are shown in Figures 2 and 3. The morphology of the membranes was not influenced by PES concentration and the membranes prepared with different concentrations of PES reveal finger-like structure. In all the cases, membranes glass (bottom) side exhibits more porous nature than air (top) side. Here, morphology of the PES membrane was influenced by [BMIM][PF6] concentration. A clear visual difference was observed in SEM analysis of PES membrane structure produced using different [BMIM][PF6] concentration. PES/[BMIM][PF6] (25wt%) membranes showed a sponge-like morphology (Membranes 5 and 14); whereas membrane prepared without IL or with lower concentration of IL (5wt%) presented a channel-like morphology (Membrane 2, 3, 10 and 12). The membrane morphology in the non-solvent induced phase separation (NIPS) is influenced by the mechanism of the coagulation process. The polymer and solvent used to prepare the dope solution, composition of the coagulation bath, temperature and the presence of additives are affecting the morphology,

Table 2: PES and PIM Membranes Characterization

Dope Solution	PES (wt%)	DMSO (wt%)	PVPK17 (wt%)	[BMIM][PF ₆] (wt%)	Thickness (µm)	Porosity (%)	CA Air Side (°)	CA Glass Side (°)	Bubble point (bar)	Mean Pore (µm)
1	10	90	0	0	203±8	85,9±0,1	65,3±0,6	64,1±3,0	0,76±0,13	0,03±0,01
2	10	88	2	0	220±11	84,3±0,2	66,5±2,1	60,3±1,7	0,44±0,06	0,03±0,02
3	10	83	2	5	218±4	83,5±0,3	55,7±1,2	46,7±1,7	0,30±0,01	0,05±0,02
4	10	73	2	15	224±9	85,2±0,4	55,8±2,8	50,9±3,5	0,28±0,01	0,05±0,01
5	10	63	2	25	174±8	83,4±0,1	-	-	0,30±0,01	1,34±0,04
6	10	86	4	0	223±9	81,5±1,1	65,9±1,0	64,5±1,7	0,28±0,01	0,05±0,01
7	10	81	4	5	202±18	83,3±0,1	66,0±0,7	63,0±3,0	0,29±0,01	0,04±0,01
8	10	71	4	15	192±17	82,4±0,4	-	-	0,27±0,04	0,06±0,01
9	10	61	4	25	200±14	83,4±1,0	-	-	0,22±0,02	0,92±0,07
10	15	85	0	0	201±9	79,1±0,6	66,7±1,0	65,8±2,5	3,36±0,10	1,24±0,02
11	15	83	2	0	196±19	79,2±0,3	62,4±2,6	53,6±1,8	2,22±0,13	0,02±0,01
12	15	78	2	5	234±6	78,7±0,4	66,2±1,6	60,9±1,2	2,12±0,08	0,05±0,03
13	15	68	2	15	207±15	79,2±0,3	47,4±2,1	42,4±2,9	2,28±0,04	0,03±0,01
14	15	58	2	25	178±12	79,4±0,3	67,3±0,9	56,3±1,6	2,16±0,05	0,03±0,01
15	15	81	4	0	235±3	78±0,1	55,3±1,2	49,2±5,2	2,05±0,31	0,03±0,01
16	15	76	4	5	225±9	79,6±0,4	62,9±1,7	57,6±2,1	1,82±0,12	0,04±0,02
17	15	66	4	15	213±18	78,9±0,1	47,1±1,9	40,3±5,2	2,00±0,25	0,03±0,01
18	15	56	4	25	219±18	78,1±0,1	-	-	0,49±0,18	0,39±0,04

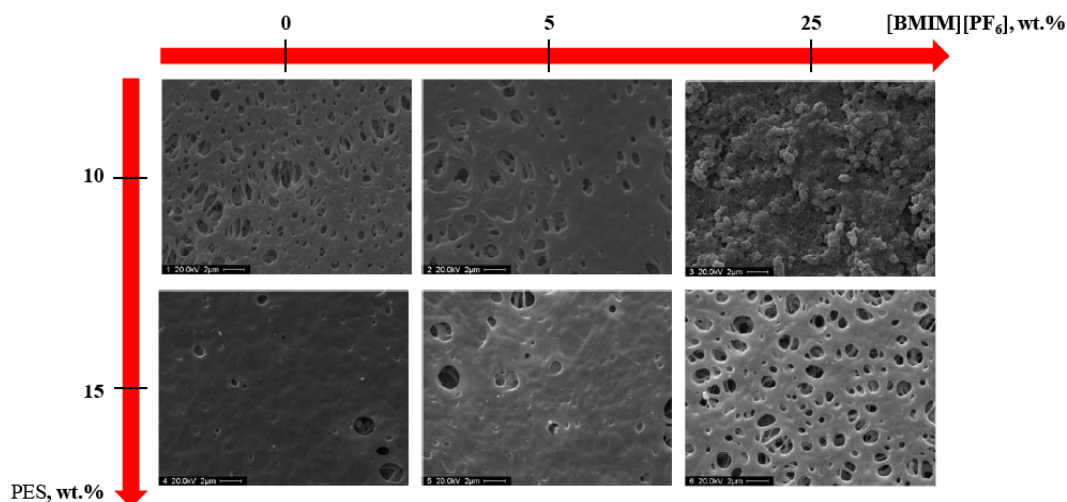


Figure 2: SEM images of the PES membrane surface, from left to right: blank PES, PES/5 wt% [BMIM][PF₆], PES/25 wt% [BMIM][PF₆].

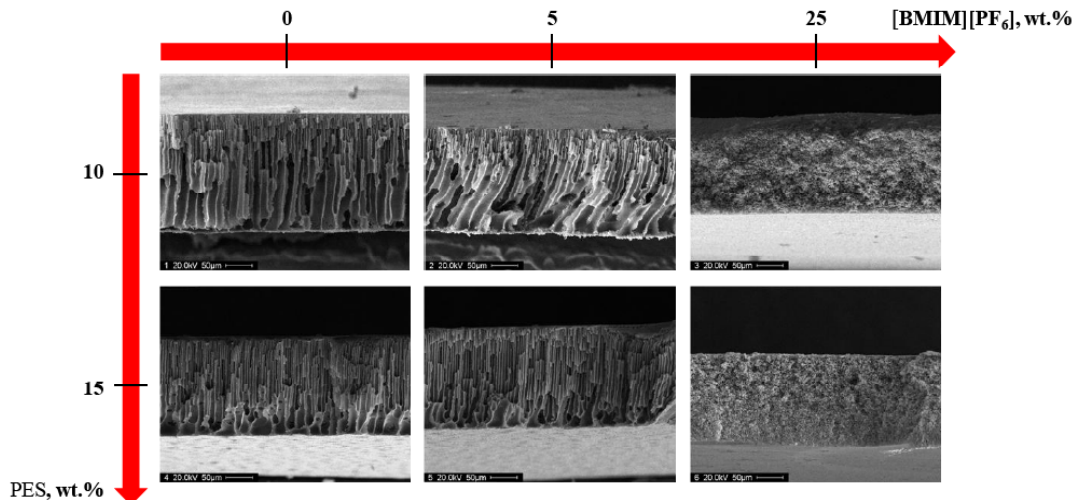


Figure 3: SEM images of the PES membrane cross section, from left to right: blank PES, PES/5 wt% [BMIM][PF₆], PES/25 wt% [BMIM][PF₆].

because of their noted influence on the solvent/non-solvent exchange velocity. The change of morphology can be explained through the viscosity of the dope solution too. [BMIM][PF₆] concentration in the PES/DMSO dope solution influences the total viscosity and consequently alters the phase inversion kinetics and morphology. At low IL concentrations, finger-like morphologies with high voids were observed as a consequence of the faster rate of solvent-non-solvent exchange and rapid demixing rate during the phase inversion process. Whereas at higher [BMIM][PF₆] concentration the viscosity of the dope solution dramatically increased and as consequence, the demixing was delayed and a sponge-like structure obtained.

3.1.2. Membrane Thickness and Porosity

The thicknesses of the produced membranes are in the range of 180 - 225 μ m and PES concentration does not influence it, whereas addition of PVPK17 in the dope solution slightly increases the thickness as expected. PES membranes prepared exhibit high porosity in the range of 79% to 86%. As shown in Figure 4, in all the cases, the membranes prepared by casting a dope solution containing 15wt% PES exhibit higher porosities than membranes with 10wt% PES. The increase of PVPK17 concentration slightly decreases the porosity of PES membranes, whereas porosity was not influenced by the IL concentration (Figures 4 and 5).

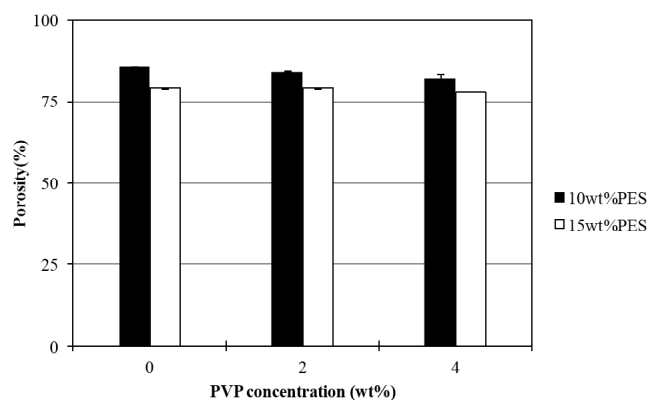


Figure 4: Porosity of PES membrane as a function of PVPK17 concentration.

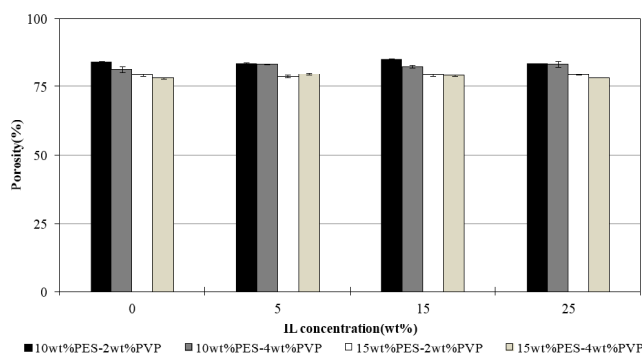


Figure 5: Porosity of PES membrane as a function of IL concentration.

3.1.3. Contact Angle

The hydrophilicity of the membrane is confirmed by contact angle measurements, and the values of both the surface (glass and air side) of PES membrane are lower than 90° (in the range from 47° to 67°). In all cases, the glass surface is more hydrophilic than the air surface, and this phenomenon may be due to the different distribution of additives throughout the PES network (Table 2). The contact angle of membranes is not influenced much by the PVPK17 concentration. On the contrary, the hydrophilicity of PES membranes is influenced by the concentration of IL. When the [BMIM][PF₆] concentration increased from 15wt% to 25wt%, the contact angle of the membrane dramatically decreased. Particularly, Membrane 5, 8, 9 and 15 (as shown in Table 1) were so hydrophilic that the water drop was absorbed in few seconds, and it was unable to measure the static contact angle.

3.1.4. Bubble Point

The effect of the additives PVPK17 and [BMIM][PF₆] on bubble point was reported (Figures 6-7). Comparing the bubble point of the membrane without any additive, 10wt% PES membranes showed

a lower bubble point than 15wt% PES. When the PES concentration was increased from 10wt% to 15wt%, the bubble point increased from 0.8bar to 3.4bar. As consequence, the size of the pores decreased from $0.8\ \mu\text{m}$ to $0.2\ \mu\text{m}$. Whereas, increasing PVPK17 concentration, from 0wt% to 4wt%, the bubble point decreased while the size of the largest pore on membrane surface increased (Figure 6). In the case of a [BMIM][PF₆] concentration in the range of 0-15wt%, no evident influence on the bubble point was reported, and membrane cross-section showed finger-like channels. Clear differences were observed at IL concentration of 25wt%, the bubble point strongly decreased and the membrane morphology changed from finger-like to sponge-like (Figure 7).

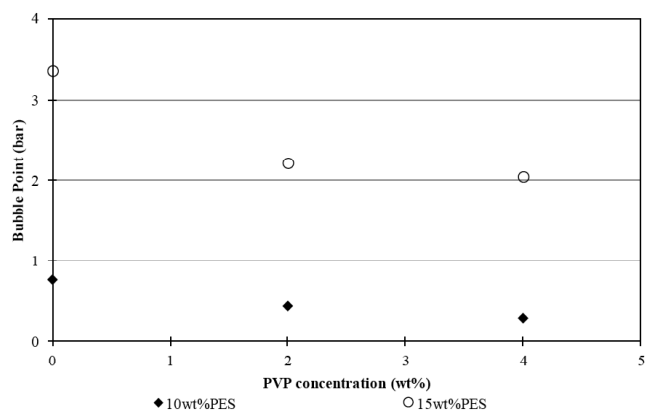


Figure 6: Bubble point of PES membrane as a function of PVPK17 concentration.

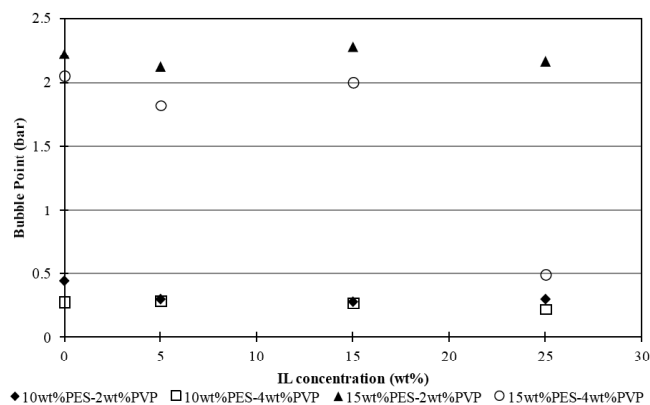


Figure 7: Bubble point of produced PES membrane as a function of [BMIM][PF₆] concentration.

3.1.5. Membrane Pore Size

It is observed from Figure 8, that PVPK17 concentration increases the pore size. The membrane prepared with higher PES concentration (15wt%) showed lower pore size than with 10wt% of PES. Bubble point and pore size results confirmed that the

influence of PVPK17 on the pore size of the membranes. The mean pore size of membranes was not influenced much when the IL concentration is lower than 15wt%. Once the [BMIM][PF₆] concentration is at 25wt% the mean pore size significantly increased. The influence of PVPK17 concentration on water permeability at different feed pressure (from 0.5 bar to 1.5 bar) is shown in Figure 9.

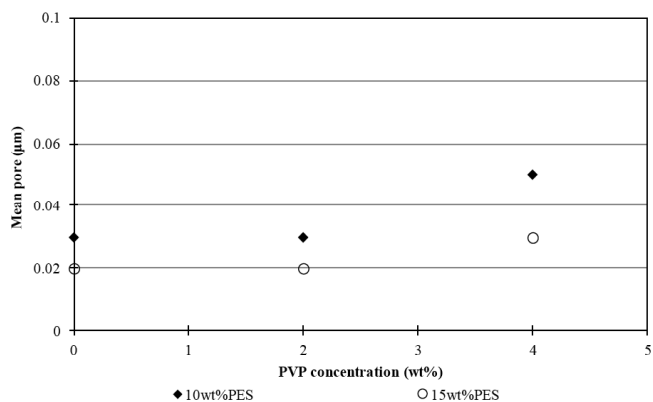


Figure 8: Mean pore of produced PES membrane as a function of PVPK17 concentration.

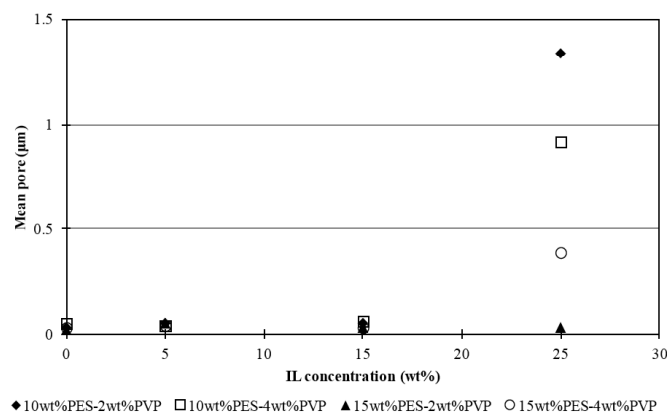


Figure 9: Mean pore of produced PES membrane as a function of [BMIM][PF₆] concentration.

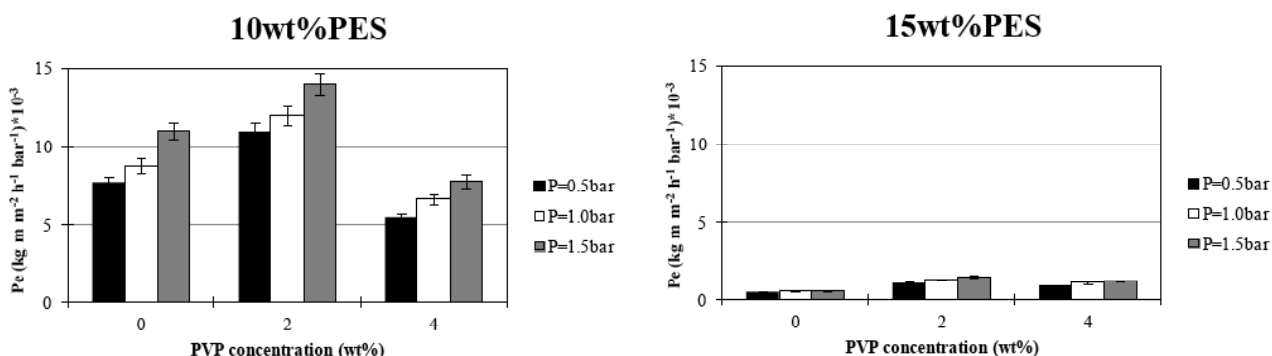


Figure 10: Influence of PVPK17 concentration on water permeability of PES membranes.

3.1.6. Membrane Permeability

The increase of the feed pressure, from 0.5 to 1.5bar, determines an increase of the water permeability of the membranes, as expected. Membrane permeability decreased with the increase of PES concentration from 10wt% to 15wt%, also depends on porosity and pore size of membranes. As reported in Figures 4 and 5, the increase of PES concentration from 10wt% to 15wt% decreased the porosity and pore size of the membrane and consequently the water permeability. The addition of 2wt% of PVPK17 increased the pore size and the water permeability. Whereas, increasing the PVPK17 concentration up to 4wt% the water permeability decreased significantly. The reason may be due to the incomplete PVPK17 removal during the membrane post-treatment; PVPK17 partially remained in the PES matrix surface and reduced the porosity of the membranes (Figure 10). In fact, in the case of membranes prepared with 10wt% PES and PVPK17 concentration of 4wt%, a decrease of the porosity from 86% to 81% was observed with consequently reduced permeability from $7.7 \cdot 10^{-3} \text{ kg m}^{-2} \text{ h}^{-1} \text{ bar}^{-1}$ to $5.5 \cdot 10^{-3} \text{ kg m}^{-2} \text{ h}^{-1} \text{ bar}^{-1}$. Membranes with high porosity and larger pore size are preferable as adsorbents because of their higher membrane contact area. For this reason, membranes prepared with 10wt% PES and 2wt%PVPK17 were selected for RB19 dye adsorption batch tests by their higher porosity.

3.1.7. Test of RB19 Dye Adsorption in Batch System

Membranes with 10wt% PES-2wt% PVPK17 and different [BMIM][PF₆] concentrations, from 5wt% to 25wt%, were used in dye adsorption batch tests. The operative conditions used in the experiments are summarized in Table 3.

Table 3: Test of RB 19 Dye Adsorption in Batch

Experiment N°	[BMIM][PF ₆] (wt%)	Membrane weight (g)	pH	Remazol Brilliant Blue R (ppm)
1	5	0,02	3	10
2	5	0,04	7	20
3	5	0,06	10	30
4	15	0,02	7	30
5	15	0,04	10	10
6	15	0,06	3	20
7	25	0,02	10	20
8	25	0,04	7	30
9	25	0,06	3	10

The experiments confirmed that PES membranes loaded with [BMIM][PF₆] could be used as adsorbents for dye removal from aqueous solution. In fact, the adsorption was in the range of 17-64%. The experiments confirmed that the performance of PIMs depends on the amount of adsorbent, pH and dye concentration.

The degree of dye removal increases, as expected, with the increase of the amount of adsorbent [57]. The PIMs adsorbed higher percentage of RB19 when the dye concentration was lower. The performance of the RB19 removal test was also influenced by the solution pH and PES/[BMIM][PF₆] membranes showed a better adsorption at higher pH range. From the earlier research studies, it was found that pH of aqueous solution significantly influences the degree of ionization of a dye molecule. When [BMIM][PF₆] is used as an organic phase, the sulfonate groups of RB19 are dissociated into an anionic form forming hydrogen bonding with [BMIM][PF₆]. On the other hand, in alkaline (higher pH conditions) RB19 solution there is a considerable decrease in adsorption efficiency, suggesting the role of hydrogen-bonding interaction in the extraction of different species of the anionic dyes. In fact, a desirable hydrogen bonding could be formed between anionic species (sulfonated group) of RB19 and the acidic 2H of imidazolium cation of the ILs compared. Pei *et al.* [30] reported that the hydrophobic interactions between azo dyes and the ILs also drive the transfer of the azo dyes from water to the ILs phase as well.

By these results, the performance of dye removal experiment was optimized according to four variables *i.e.* initial dye concentration, pH, IL concentration, and membrane weight. The optimization process was carried out by the multivariate approach of "Experiment Design". An experimental design can be considered as

a series of experiments that, in general, are defined a priori and allow evaluating the influence of a predefined number of factors in a predefined number of experiments. Although several experimental designs with specific features are available, in this study a central composite design (CCD) consisting of a 24 factorial design with six-star points positioned at $\pm\alpha$ from the center of the experimental domain was chosen. CCD allows the linear effects, the interactions between pairs of variables and the quadratic effects to be estimated. The axial distance α was chosen as 2 to establish the rotatability condition. In this way, the design generates information uniformly in all directions, *i.e.*, a rotation of the design about the origin does not alter the variance contours. In total, the experimental design matrix had 30 runs [24+(2×4)+6], six of them in the central point and the adsorption after 19 h (R% (19h)) was chosen as a response. The range of the parameters affecting the response were determined by performing preliminary tests and, according to these experiments, IL concentration in the range 5-25wt%, membrane weight 0.02-0.06 mg, pH 3-11, and finally 10-30 ppm for dye concentration were selected. Table 4 shows the design matrix in which the order of the experiments was fully randomized. The trends of the considered variables can be simply evaluated by looking at corresponding response surfaces (Figure 12). The experiments confirm that the degree of dye removal increases with the increase of the amount of adsorbent, as expected, and the PIMs adsorbed higher percentage of RB19 when the dye concentration was lower. Finally, the performance of the test of RB19 removal is influenced by the pH and, in particular, PES membrane [BMIM][PF₆] showed elevated adsorption when the pH was lower. The optimum working conditions that can be deduced by examining graphics were the following: IL concentration 10.7wt%, membrane weight 0.055 mg, pH 3.0, dye concentration 10.0 ppm.

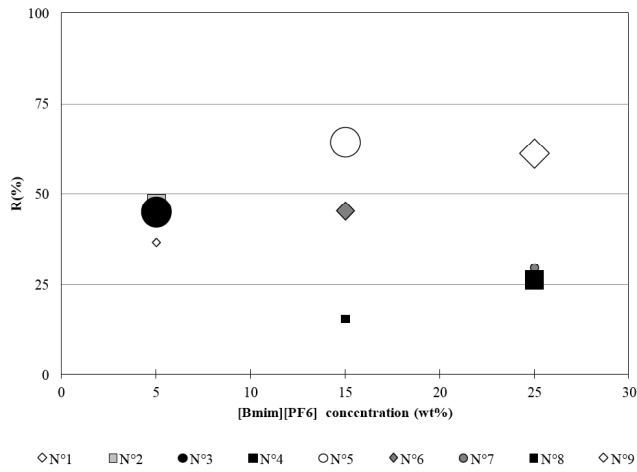


Figure 11: Effect of RB 19 dye adsorption at different experimental conditions.

Studies on the kinetic of the dye removal were carried out in the optimized operating conditions by monitoring the adsorption Vs time (24 hr) (Figure 13). The experiment showed that the adsorption is a function of the contact time of the adsorbent with the contaminated water solution. In fact, the degree adsorption of RB19 increased during the time until achieving a maximum value (R~69%) at 1200min due to the saturation of the absorptive capacity of the PIMs. The adsorption process of RB19 was then evaluated by carrying out an experiment at optimized conditions, and the experimental adsorption percentage value (69.2%) was in agreement to those predicted by the CCD model (71.7%).

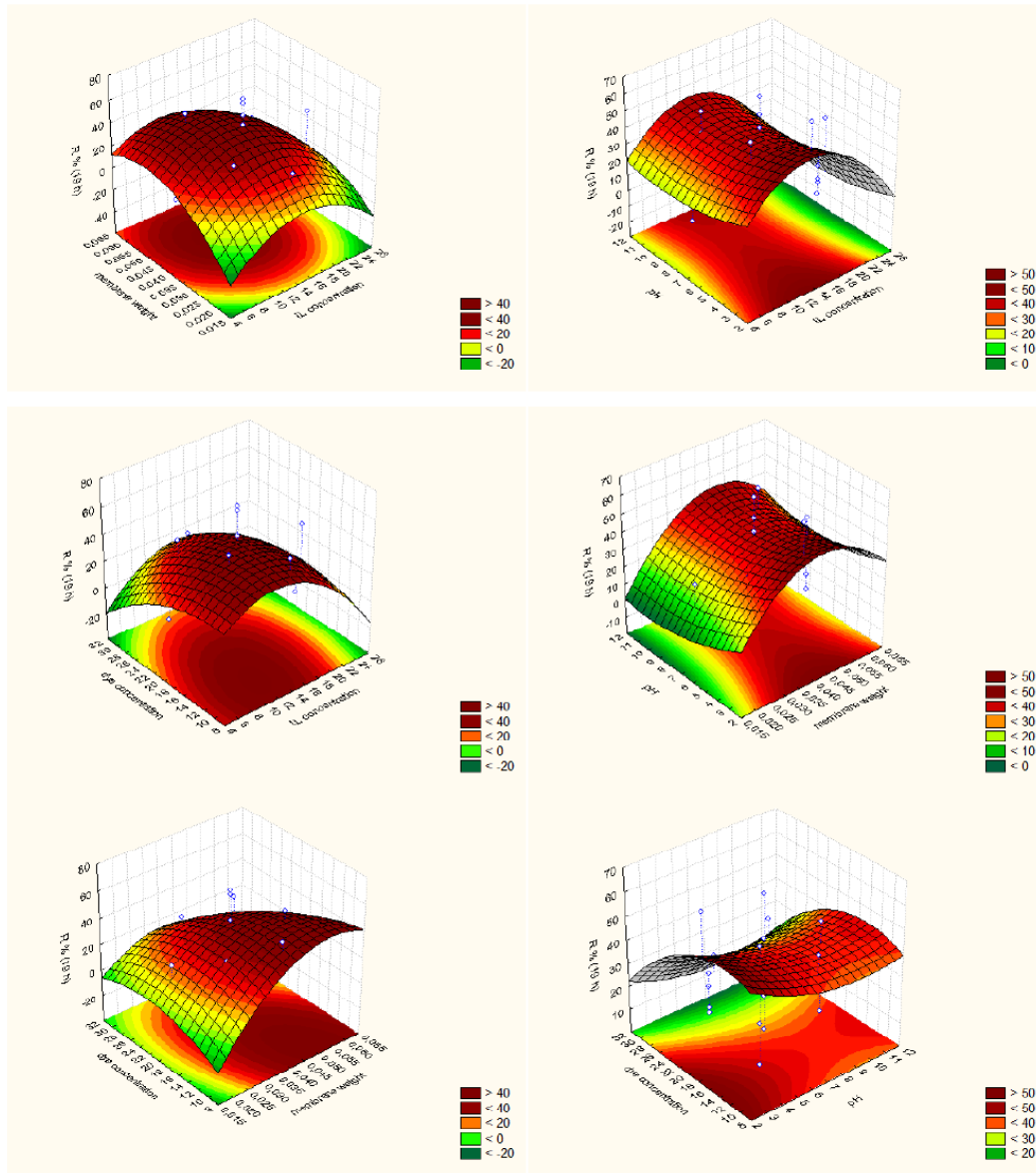


Figure 12: Response surfaces obtained from the central composite design.

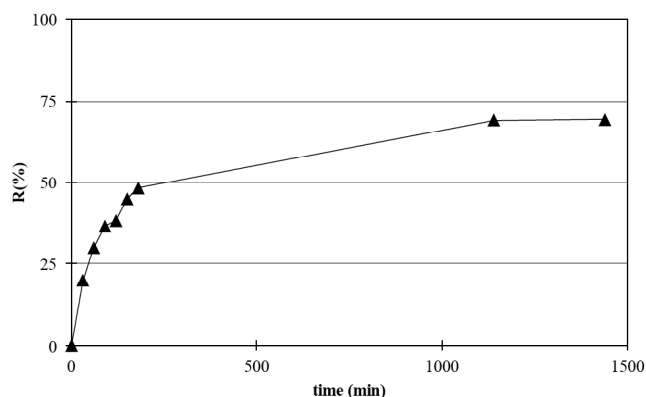


Figure 13: RB 19 dye adsorption at optimal experimental conditions.

Adsorption is an inexpensive and energy saving process for dye removal from wastewater. Several innovative materials (*i.e.* ILs), nanoparticles or activated carbon consent a degree of dye removal higher than 90% (Chan, 2008; Pei, 2007; Shanehsaz, 2015). Nevertheless, the separation of the activated carbon from the wastewater after adsorption is one of the critical issue of this process. Whereas in the case of PIMs, the recovery and reuse of the absorbent materials (ionic liquids) is quite easy due to its inclusion in the PES membrane matrix. However, a decrease of the removal efficiency of the IL in the polymer is observed and this is due to the PES matrix which hindering the adsorption of the dye by the entrapped ILs.

Table 4: Matrix of the Central Composite Experimental Design for the Optimization of the Variables Affecting Adsorption Process and the Obtained Responses (R% (20 hr))

Exp.No	IL Concentration (wt%)	Membrane Weight (mg)	pH	Dye Concentration (ppm)	Response (R% (20hr))
25 (C)	15	0.04	7	20	43.4
1	10	0.03	5	15	34.6
10	20	0.03	5	25	10
29 (C)	15	0.04	7	20	33
17	5	0.04	7	20	4.5
28 (C)	15	0.04	7	20	35.5
15	20	0.05	9	15	23.9
11	20	0.03	9	15	13.6
21	15	0.04	3	20	65.5
13	20	0.05	5	15	20.5
30 (C)	15	0.04	7	20	43.5
9	20	0.03	5	15	2.7
18	25	0.04	7	20	31.3
23	15	0.04	7	10	51
5	10	0.05	5	15	52.9
27 (C)	15	0.04	7	20	62.1
16	20	0.05	9	25	10.2
12	20	0.03	9	25	7.4
6	10	0.05	5	25	27
19	15	0.02	7	20	28.6
22	15	0.04	11	20	35
4	10	0.03	9	25	25
24	15	0.04	7	30	22.2
2	10	0.03	5	25	21.5
7	10	0.05	9	15	52.4
3	10	0.03	9	15	26.3
8	10	0.05	9	25	39.7
14	20	0.05	5	25	12.1
26 (C)	15	0.04	7	20	19
20	15	0.06	7	20	28.6

3.1.8. Future Work - Implications of ILs in Dye Effluent Treatment

In the current investigation, the results reveal that RB19 dyes used in industry can be efficiently adsorbed/separated from aqueous solution phase, using a small quantity of ionic liquid. The tunable characteristics of ILs, especially loaded in polymeric matrix module provide an additional advantage of preventing ILs loss during the adsorption process. [BMIM][PF6] solubility in water is in the ppm range, and here it is interwoven in the PES polymer matrix form. However, few major part of the follow-up research works need to be done, especially to assure the complete removal/recovery of the dye (RB19) from the PIM support and reusability of the membrane for further experiments. A comprehensive investigation is required to find a procedure for the recovery of ILs and overall engineering cost analysis of ILs-based dye separation processes.

4. CONCLUSION

Polymer inclusion membranes (PIMs) were prepared via NIPS using PES as polymeric matrix network to load ionic liquid [BMIM][PF6] and PVPK17-K17 as pore forming agent. The addition of 2wt% of PVPK17 increased the pore size of the membrane without compromising the physicochemical properties of PES membrane, such as the hydrophilicity and porosity. The addition of [BMIM][PF6] did not influence the properties of the membrane at a concentration lower than 15wt%. On the contrary, the morphology of PES membrane dramatically changed from finger to spongy type at 25wt% of IL concentration of PIMs. PIMs made of PES/2wt% PVPK17/[BMIM][PF6] were tested for RB19 dye adsorption. Moreover, the dye adsorption was influenced by the amount of adsorbent, IL concentration, pH, and dye concentration.

By the screening on the variables in RB19 adsorption experiments, the optimal operative conditions to achieve the maximum degree of dye removal are IL concentration 10.7wt%, membrane weight 0.055 mg, pH 3.0, dye concentration 10.0 ppm. Once optimized the operating conditions, the kinetic of the dye removal experiments showed that the degree of RB19 adsorption increased with time and attained a maximum value of 69.2% after 1200min.

ACKNOWLEDGMENTS

This work has been funded by the European Community's Programme (FP7-PEOPLE-IIF- 2008),

Grant Agreement No. 237855, Project ILMC. Dr. Mariano Davoli is acknowledged for the SEM pictures analysis.

REFERENCE

- [1] Paulino AT, Guilherme MR, Reis AV, Campese GM, Muniz EC, Nozaki J, Removal of methylene. *J Colloid Interface Sci* 2006; 301: 55-62.
<http://dx.doi.org/10.1016/j.jcis.2006.04.036>
- [2] Gupta VK, Suhas, Application. *J Environ Manage* 2009; 90: 2313-2342.
<http://dx.doi.org/10.1016/j.jenvman.2008.11.017>
- [3] Zaharia C, Suteu D, Textile Organic Dyes - Characteristics, Polluting Effects and Separation/Elimination Procedures from Industrial Effluents - A Critical Overview, Organic Pollutants Ten Years After the Stockholm Convention - Environmental and Analytical Update, Dr. Tomasz Puzyn (Ed. ISBN: 978-953-307), In Tech press 2012; p. 917-922.
- [4] Stydini M, Dimitris IK, Verykios XE, Visible light. *Appl Catal Environ* 2004; 47: 189-201.
- [5] Allegre C, Moulin P, Maisseu M, Charbit F, Treatment. *J Membr Sci* 2006; 269: 15-34.
- [6] Liu HL, Chiou R, Optimal decolorization. *J Chin Inst Chem Engrs* 2006; 37: 289-298.
- [7] Liu CH, Wu JS, Chiu HC, Suen SY, Chu KH, Removal of anionic. *Water Res* 2007; 41: 1491-1500.
<http://dx.doi.org/10.1016/j.watres.2007.01.023>
- [8] Gupta VK, Suhas Ali I, Saini VK, Removal of Rhodamine B, Fast green, Methylene blue. *Ind Eng Chem Res* 2004; 43: 1740-1747.
<http://dx.doi.org/10.1021/ie034218g>
- [9] Gupta VK, Ali I, Saini, VK, Van Gerven TVan der Bruggen B, Vandecasteele, C. 2005. Removal of dyes. *Ind Eng Chem Res* 2005, 44, 3655-3664.
<http://dx.doi.org/10.1021/ie0500220>
- [10] Gupta VK, Mittal A, Gajbe V, Mittal J, Removal. *Ind Eng Chem Res* 2006; 45: 1446-1453.
<http://dx.doi.org/10.1021/ie051111f>
- [11] Yahya S, Al-Degs, Musa I. El-Barghouthi, Amjad H. El-Sheikh, Gavin MW, Effect of solution pH. *Dyes and Pigments* 2007; 77: 16-23.
- [12] Dedrick RL, Beckmann RB, Kinetics. *AIChE J* 1967; 3: 68-75.
- [13] Simkovic I, Laszlo JA, Thompson AR, Preparation. *Carbohydr Polym* 1996; 30: 25-30.
- [14] Laszlo JA, Regeneration. *Environ Sci Technol* 2000; 34: 167-172.
<http://dx.doi.org/10.1021/es990918u>
- [15] Karcher S, Kornmuller A, Jekel M, Screening. *Dyes Pigments* 2001; 51: 111-125.
[http://dx.doi.org/10.1016/S0143-7208\(01\)00066-3](http://dx.doi.org/10.1016/S0143-7208(01)00066-3)
- [16] Wu FC, Tseng RL, Juang RS, Adsorption of dyes. *J Chem Technol Biotechnol* 2002; 77: 1269-1279.
<http://dx.doi.org/10.1002/jctb.705>
- [17] Tseng RL, Wu FC, Juang RS, Liquid-phase. *Carbon* 2003; 41: 487-495.
[http://dx.doi.org/10.1016/S0008-6223\(02\)00367-6](http://dx.doi.org/10.1016/S0008-6223(02)00367-6)
- [18] Chang MY, Juang RS, Adsorption. *J Colloid Interface Sci* 2004; 278, 18-25.
<http://dx.doi.org/10.1016/j.jcis.2004.05.029>
- [19] Ozdemir O, Armagan B, Turan M, Celik MS, Comparison. *Dyes Pigments* 2004; 62: 49-60.
<http://dx.doi.org/10.1016/j.dyepig.2003.11.007>
- [20] Wang CC, Juang LC, Hsu TC, Lee CK, Lee JF, Huang FC, Adsorption. *J Colloid Interface Sci* 2004; 273: 80-86.
<http://dx.doi.org/10.1016/j.jcis.2003.12.028>

- [21] Lee JW, Choi SP, Thiruvengatachari R, Shim WG, Moon H, Evaluation. *Dyes Pigments* 2006; 69: 196-203.
<http://dx.doi.org/10.1016/j.dyepig.2005.03.008>
- [22] Oren G E, Gryglewicz G, Adsorption characteristics. *Dyes Pigments* 2007; 74: 34-40.
- [23] Fakhar NM, Shahabuddin M, Calixarenes: A Versatile Source. *Pak. J Anal Environ Chem* 2012; 13: 148 - 58
- [24] Jing F, Yunchang F, Sheli Z, Jianji W, Extraction. *Sep Sci Technol* 2011; 46: 1172-1177.
- [25] Brennecke JF, Maginn EJ, Ionic liquids. *AIChE J* 2001; 47: 2384-2389.
<http://dx.doi.org/10.1002/aic.690471102>
- [26] Han D, Row KH, Recent applications. *Molecules* 2010; 15: 2405-2426.
<http://dx.doi.org/10.3390/molecules15042405>
- [27] Poole CF, Poole SK, Extraction. *J Chromato A* 2010; 1217: 2268-2286.
<http://dx.doi.org/10.1016/j.chroma.2009.09.011>
- [28] Ma J, Hong X, Application. *J Environ Manag* 2012; 99: 104-109.
<http://dx.doi.org/10.1016/j.jenvman.2012.01.013>
- [29] Figoli A, Marino T, Simone S, Di Nicolò E, Li XM, He T *et al.*, Towards non-toxic. *Green Chemistry* 2014; 11: 4034-4059.
<http://dx.doi.org/10.1039/C4GC00613E>
- [30] Pei YC, Wang JJ, Xuan XP, Fan J, Fan M, Factors affecting. *Environ Sci & Technol* 2007; 41: 5090-5095.
<http://dx.doi.org/10.1021/es062838d>
- [31] Agarwal A, Manoj, MK, Kumari S, Bagchi D, Kumar V, Pandey BD, Extractive separation. *Miner Eng* 2008; 21: 1126-1130.
- [32] Sud D, Mahajan G, Kaur MP, Agricultural waste. *Bioresour Technol* 2008; 99: 6017-6027.
<http://dx.doi.org/10.1016/j.biortech.2007.11.064>
- [33] Shanthana Lakshmi D, Cundari T, Furia E, Tagarelli A, Fioran G, Carraro M *et al.*, Preparation. *Macromol Sympo*, (Inpress November 2015).
- [34] Sastre AM, Kumar A, Shukla JP, Singh RK, Improved techniques. *Sep Purif Meth* 1998; 27: 213-298.
<http://dx.doi.org/10.1080/03602549809351641>
- [35] Vázquez MI, Romero V, Fontàs C, Anticó E, Benavente J, Polymer inclusion. *J Membr Sci* 2014; 455: 312-319
<http://dx.doi.org/10.1016/j.memsci.2013.12.072>
- [36] Almeida MI, Catrall RW, Kolev SD, Recent trends. *J Membr Sci* 2012; 415-416: 9-23.
<http://dx.doi.org/10.1016/j.memsci.2012.06.006>
- [37] Fontàs C, Tayeb R, Tingry S, Hidalgo M, Seta P, Transport of platinum (IV). *J Membr Sci* 2005; 263: 96-102.
- [38] Garcia AR, Matamoros V, Kolev SD, Fontàs C, Development of a polymer. *J Membr Sci* 2015; 492: 32-39.
- [39] Liu F, Awanis Hashim N, Liu Y, Moghareh Abed MR, Li K, Progress. *J Membr Sci* 2011; 375: 1-27
<http://dx.doi.org/10.1016/j.memsci.2011.03.014>
- [40] Kyzas GZ, Bikiaris DN, Lazaridis NK, Selective separation. *Chem Eng J* 2009; 149: 263-272.
<http://dx.doi.org/10.1016/j.cej.2008.11.002>
- [41] Luo X, Zhan Y, Huang Y, Yang L, Tu X, Luo S, Removal of water. *J Hazard Mater* 2011; 187: 274-282.
<http://dx.doi.org/10.1016/j.jhazmat.2011.01.009>
- [42] Aitali S, Polymer Inclusion Membrane. Oral AY, Oral ZB, editors. *Proceedings of the Intern 2015, 3rd International Multidisciplinary Microscopy And Microanalysis*; 2015: Turkey, October 19-23
- [43] Aitali S, Anionic dye. Oral AY, Oral ZB, editors. *Proceedings of the Intern2015, 3rd International Multidisciplinary Microscopy And Microanalysis*; 2015: Turkey, October 19-23
- [44] Vesna VP, Sanja S, Aleksandra RN, Sava JV, Adsorption of azo dyes. *Hem Ind* 2013; 67: 881-900
<http://dx.doi.org/10.2298/HEMIND121203020P>
- [45] Aitali S, Kebiche SO, Mansouri L, Benamor M, Cationic dye. *Procedia Eng* 2012; 33: 38-46. ISSN: 1877-7058
- [46] Mansoureh ZM, Alireza B, Abdollah RM, Ionic liquid functionalized nanoporous silica for removal of anionic dye. *J Mol Liq* 2013; 180: 95-100.
<http://dx.doi.org/10.1016/j.molliq.2013.01.007>
- [47] Vijayaraghavan R, Vedaraman N, Surianarayanan M, Mac Farlane DR, Extraction. *Talanta* 2006; 69: 1059-1062.
<http://dx.doi.org/10.1016/j.talanta.2005.12.042>
- [48] Li C, Xin B, Xu W, Zhang Q, Study on extraction. *J Chem Technol Biotechnol* 2006; 85: 196-204.
- [49] Changping L, Baoping X, Wenguo X, Qi Z, Study on the extraction. *J Chem Technol Biotechnol* 2007; 82: 196-204
- [50] Maysam G, Farzaneh S, A novel method. *Clean Soil Air Wat* 2012; 40: 290-297.
- [51] Kurniawan TA, Chan GYS, Lo WH, Babel S, Physico-chemical. *Chem Eng J* 2006; 118: 83-98.
<http://dx.doi.org/10.1016/j.cej.2006.01.015>
- [52] Xu ZL, Alsahy QF, Polyethersulfone. *J Membr Sci* 2004; 233: 101-111
<http://dx.doi.org/10.1016/j.memsci.2004.01.005>
- [53] Cheryan M. *Ultrafiltration and Microfiltration Handbook*, Technomic Publishing Co., Lancaster, PA, 1998.
- [54] Wang K, Chung T, Gryta M, Hydrophobic. *Chem Engg Sci* 2008; 63: 2587-2594.
- [55] Feng CS, Shi, B, Li, G, Preparation. *J Membr Sci* 2004; 237: 15-24.
<http://dx.doi.org/10.1016/j.memsci.2004.02.007>
- [56] Chan LS, Cheung WH, McKay G, Adsorption of acid. *Desalination* 2008; 218: 304-312.
<http://dx.doi.org/10.1016/j.desal.2007.02.026>
- [57] Shanehsaz M, Seidi S, Ghorbani Y, Shoja SMR, Rouhani S, Polypyrrole. *Spectrochimacta Part A: Mol Biomol Spectros*. 2015; 149: 481-486
<http://dx.doi.org/10.1016/j.saa.2015.04.114>
- [58] Sung WW, Min HH, Yeoung SY, Different binding. *Water Res* 2008; 42: 4847-4855
- [59] Aitali S, Senhadji O, Oughlis F, Benamor M, Equilibrium and kinetic *Desal Wat Treatm* 2014; 1-12